nature physics

LETTERS

PUBLISHED ONLINE: 20 MAY 2012 | DOI: 10.1038/NPHYS2324

# Efficient and long-lived quantum memory with cold atoms inside a ring cavity

Xiao-Hui Bao[1,2], Andreas Reingruber[1], Peter Dietrich[1], Jun Rui[2], Alexander Dück[1], Thorsten Strassel[1], Li Li[2], Nai-Le Liu[2], Bo Zhao[2]* and Jian-Wei Pan[1,2]*

**Quantum memories are regarded as one of the fundamental building blocks of linear-optical quantum computation[1] and long-distance quantum communication[2]. A long-standing goal to realize scalable quantum information processing is to build a long-lived and efficient quantum memory. There have been significant efforts distributed towards this goal. However, either efficient but short-lived[3,4] or long-lived but inefficient quantum memories[5–7] have been demonstrated so far. Here we report a high-performance quantum memory in which long lifetime and high retrieval efficiency meet for the first time. By placing a ring cavity around an atomic ensemble, employing a pair of clock states, creating a long-wavelength spin wave and arranging the set-up in the gravitational direction, we realize a quantum memory with an intrinsic spin wave to photon conversion efficiency of 73(2)% together with a storage lifetime of 3.2(1) ms. This realization provides an essential tool towards scalable linear-optical quantum information processing.**

A high-performance quantum memory is of crucial importance for large-scale linear-optical quantum computation[1], distributed quantum computing and long-distance quantum communication[2]. The lifetime and the retrieval efficiency of a quantum memory are two important quantities that determine the scalability of realistic quantum information protocols. For a certain quantum information task, for example creating a large-scale cluster state[8] or distributing entanglement through the quantum repeater protocol[9–12], the time overhead $T_r$ is inversely proportional to a power law of the retrieval efficiency $R$, $T_r \propto R^{-n}$, where $n$ is determined by the scale of the quantum computation or the communication distance. To implement one of those tasks, the lifetime of the quantum memory must be larger than this time overhead. To satisfy this condition, one has to improve the lifetime of the quantum memory and reduce the time overhead by improving the retrieval efficiency. Besides, different protocols also set thresholds on the retrieval efficiency and lifetime. For example, in loss-tolerant linear-optical quantum computation the minimum retrieval efficiency required is 50% (ref. 13) and in long-distance quantum communication distributing entanglement over 1,000 km requires a communication time of at least 3.3 ms.

Quantum memories for light have been demonstrated with atomic ensembles[14–16], solid-state systems[17,18] and single atoms[19]. With these quantum memories, the principles of some quantum information protocols have been demonstrated, for example, functional quantum repeater nodes were realized with atomic ensembles[20,21]. However, owing to the low retrieval efficiency and short lifetime, the implementation of further steps is extremely difficult. Therefore, in recent years, many efforts have been devoted towards improving the retrieval efficiency and the lifetime of quantum memories and significant progress has been achieved. However, an efficient and long-lived quantum memory remains challenging. For example, the lifetime of the atomic quantum memory has been experimentally improved to the millisecond regime either by increasing the spin wave wavelength[5] or confining the atoms in an optical lattice[6,7], but the intrinsic retrieval efficiency is less than 25%. Efficient quantum memories have been demonstrated in atomic[3] and solid-state media[4], reaching retrieval efficiencies up to 84% and 69%, respectively. However, the observed lifetimes were severely limited (240 ns and 3 μs respectively). The inability to achieve both long lifetime and high retrieval efficiency in a single quantum memory strongly limits more advanced operations, such as creating or purifying entanglement[22] between two or more quantum repeater nodes or entangling six atomic ensembles to generate Greenberger–Horne–Zeilinger states, which are the building blocks of linear-optical quantum computing[23], and thus is one of the present bottlenecks hindering the implementation of scalable quantum information processing.

Here, we report an atomic-ensemble quantum memory that has a long lifetime and a high retrieval efficiency simultaneously. To achieve this challenging goal, we employ a ring cavity to enhance the write and read processes through the Purcell effect, use a pair of clock states to suppress magnetic-field-induced decoherence and design the directions of the classical beams and single-photons to be collinear to obtain a spin wave with the maximal wavelength. We also design the set-up and detection beams to be in the direction of gravity to maintain a good overlap between the control beams and the atomic ensemble during the free fall. By making these improvements, we have managed to achieve a quantum memory with an initial intrinsic retrieval efficiency of 73(2)% and a $1/e$ lifetime of 3.2(1) ms.

The experimental set-up is shown in Fig. 1. An atomic ensemble composed of $\sim 10^8$ $^{87}$Rb atoms, prepared by a magneto-optical trap (MOT) with subsequent molasses cooling, serves as a quantum memory. Initially, the atoms are in the ground state $|g\rangle$. During the write process a single-quanta spin wave is imprinted on the atomic ensemble conditioned on the detection of a spontaneously emitted write-out photon (in the same spatial mode as the write beam). By applying the read beam after a controllable delay, the spin wave is converted back into a read-out photon. To improve the retrieval efficiency, a ring cavity with a finesse of 48(1) is placed around the vacuum chamber to increase the effective optical depth. The cavity mode is aligned to overlap with the centre of the atomic ensemble. The use of a ring cavity allows us to distinguish the

[1]Physikalisches Institut der Universitaet Heidelberg, Philosophenweg 12, Heidelberg 69120, Germany, [2]National Laboratory for Physical Sciences at Microscale and Department of Modern Physics, University of Science and Technology of China, Hefei, Anhui 230026, China. *e-mail: bozhao@ustc.edu.cn; pan@ustc.edu.cn.

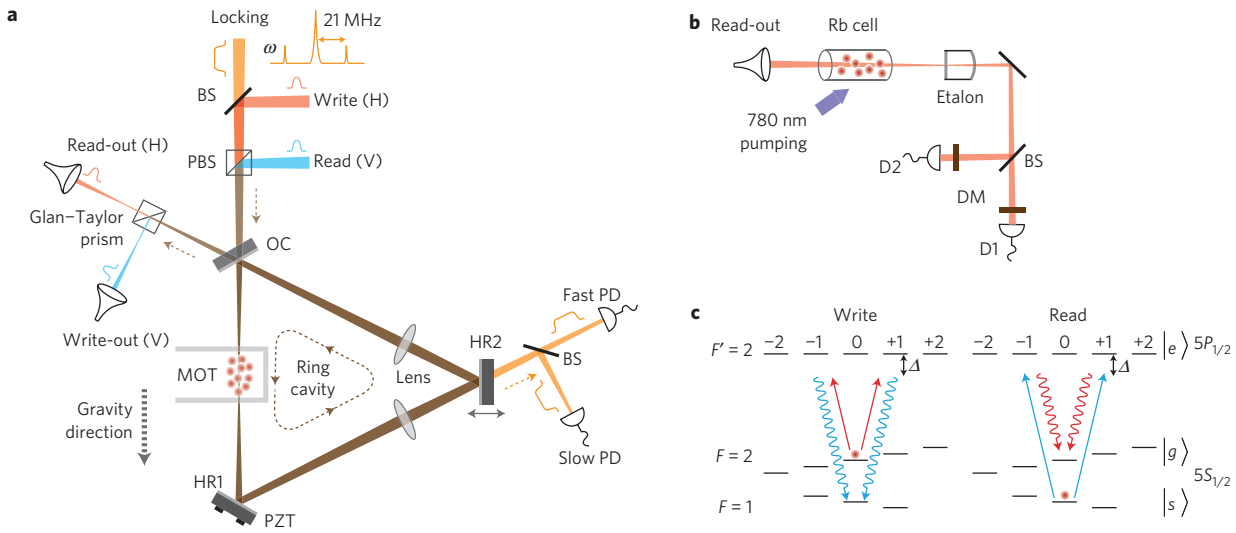


**Figure 1 | Experimental set-up and level scheme. a**, A ring cavity is built outside a vacuum glass cell with an anti-reflection coating. It mainly consists of two highly reflecting mirrors (HR1 and HR2) and an output coupler (OC). HR1 is mounted on a piezoelectric transducer (PZT) for the active stabilization of the cavity length. HR2 is mounted on a manual translation stage to change the cavity FSR. The write is horizontally (H) polarized and the read is vertically (V) polarized relative to the ring-cavity plane. These two control beams are combined with a polarizing beam splitter (PBS) and coupled into the cavity through the output coupler. Write-out and read-out photons are collected in the other port of the output coupler. A frequency-modulated locking beam, which is blue-detuned by the cavity's FSR, is combined with the write through a nonpolarizing beam splitter (BS). Leakage of the locking beams through HR2 is measured with a fast and a slow photodiode (PD) to create the error signal for the cavity length stabilization. **b**, Filtering of read-out photons from the read beams is realized by making use of a Glan–Taylor prism (in **a**), a pumped Rb vapour cell and an etalon. Dichroic mirrors (DM) are used to remove the leakage of the vapour cell pumping beams. Finally, the read-out photons are detected with single-photon detectors (D1 and D2). The set-up for filtering write-out photons from write is the same as the read-out channel (not shown). **c**, Λ-type level scheme used. Both the write and read beams are red-detuned by $\Delta = 40$ MHz.

back-scattered from forward-scattered write-out photons, so that we can select only the forward-scattered photons and obtain a long-wavelength spin wave that is robust against dephasing caused by the atomic random motion.

In our experiment, we design the system in such a way that the frequency and polarization of the write (read) and read (write)-out photons are the same and that the cavity supports and enhances all of the four light fields. We stabilize the cavity intermittently using the Pound–Drever–Hall locking scheme during the MOT loading phase. The phase shift of the write pulse and the read-out photon caused by the atomic ensemble is compensated by slightly shifting the locking point. Leakage of the classical write and read pulses into the single-photon channels is attenuated by a factor of $\sim 10^{10}$ with three stages of filtering elements shown in Fig. 1a,b. As the write and read are configured to be co-propagating, a very high extinction ratio ($>10^{11}$) is required for the pulse switching of the write, read and the locking beam. This is realized by making use of a double-pass acousto-optic modulator (AOM) and a single-path AOM together for each of these three beams.

We first demonstrate that the use of the ring cavity preserves the quantum nature of the atomic memory but significantly enhances the retrieval efficiency. We measure the excitation probability, cross-correlation and physical retrieval efficiency for a series of write pulses of different intensities, with the results shown in Fig. 2a,b, respectively. We find the excitation probability increases linearly with the write power, indicating that the write process is within the spontaneous regime all over the measurement range. We measure the cross-correlation between the write-out and read-out photons, which is defined as $g_c^{(2)} = p_{w,r}/(p_w\, p_r)$, where $p_w$ ($p_r$) denotes the write (read)-out photon probability and $p_{w,r}$ the coincidence probability[24]. As depicted in Fig. 2a, $g_c^{(2)}$ is well above 2, which implies that the storage is in the quantum regime and the read-out photon is non-classically correlated with the write-out photon[5,25]. The probability of detecting a read-out photon conditional on a write-out photon event is $R = p_{w,r}/p_w$, whose value ranges from 12% to 22%, as shown in Fig. 2b. The calibrated retrieval efficiency is calculated by taking into account the background noise $p_{bg}$ (see Methods for details) and the total detection efficiency, as $R^c = R/[\eta_{tot}(1 - p_{bg}/p_w)]$, where the total detection efficiency $\eta_{tot} = \eta_{esp}\, \eta_t\, \eta_{spd}$ consists of the fraction of light that escapes from the output coupler $\eta_{esp} = 71(2)\%$, the propagation efficiency from the cavity to the detectors (D1 and D2 in Fig. 1) $\eta_t = 39.5(4)\%$ and the quantum efficiency of single-photon detectors $\eta_{spd} = 62.7\%$. By subtracting the random coincidence, we obtain the intrinsic retrieval efficiency $\chi = R^c(1 - 1/g_c^{(2)})$, which is shown as a function of the excitation probability in Fig. 2b. Note that $R^c$ is often used as the intrinsic retrieval efficiency in previous experiments and here we explicitly distinguish between $R^c$ and $\chi$. Over the whole measurement range, $\chi$ approximately stays constant. The calculated average value of $\chi$ is 85(3)%, which is the highest conversion efficiency of a quantum memory working at the single-photon level so far.

Next, we study the influence of the read power on the retrieval efficiency. An example of the read-out photon shape is shown in the inset of Fig. 3a. Experimentally, we find that the pulse width of the read-out photon strongly depends on the read power. With the read power increasing, the pulse width becomes narrower. This is consistent with the electromagnetically induced transparency theory[26], which predicts that the group velocity of the read-out photon should be inversely proportional to the read intensity. The measured relation is plotted in Fig. 3a and fitted with the function $a/I_r + \tau_0$ where $I_r$ is the read power and $a$ is a free parameter The fitted result for $\tau_0 = 38.9 \pm 1.3$ ns is mainly limited by the cavity decay time (8.9 ns) and the rise time of the read pulse (~21 ns). We also measure the conversion efficiency $\chi$ as a function of the read power, with the results shown in Fig. 3b. We note that, except for the first two points, $\chi$ nearly stays constant over the whole measurement range. The variation of the first two points can be explained as a result of the comparable pulse width of the read and read-out pulses,

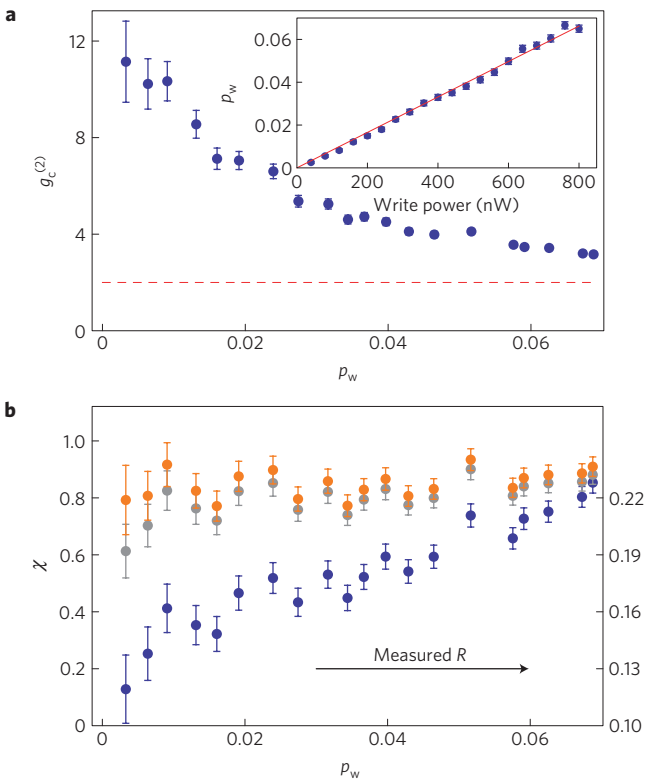


**Figure 2 | Influence of the write power. a**, Cross-correlation as a function of the excitation probability, with the inset showing the relation between excitation probability and the write power. $g_c^{(2)} > 2$ (above the dashed line) implies non-classical correlation. **b**, Intrinsic conversion efficiency $\chi$ (with $p_{bg}$ subtraction in orange, without $p_{bg}$ subtraction in grey) and conditional retrieval efficiency $R$ (blue) as a function of the excitation probability. Data in **a**,**b** are measured in the correlation mode (see Methods for details) with a read–write delay of 500 ns. Error bars are derived on the basis of the Poisson distribution of the detector counts.

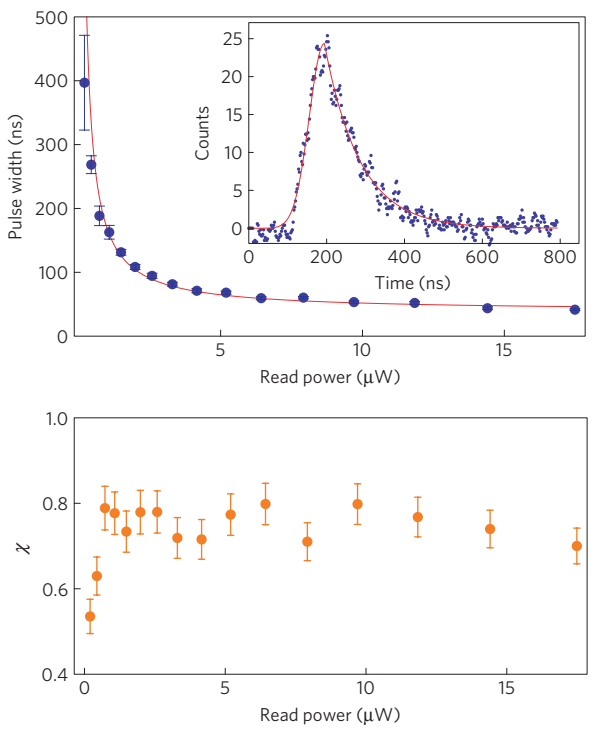


**Figure 3 | Influence of the read power. a**, Relation between the pulse width (full-width at half-maximum) and the read power, with the inset showing the pulse shape of the read-out photon with a read power of 2 μW. **b**, Intrinsic conversion efficiency $\chi$ as a function of the read power. During the measurements (**a**,**b**), the width of the read pulse is set to 700 ns. Error bars are derived on the basis of the Poisson distribution of the detector counts.

which leads to an incomplete read-out process. This implies that we can tune the pulse width for the read-out photon without sacrificing the conversion efficiency. This tunability is of crucial importance for quantum communication and distributed quantum computing[27,28] because it is usually required to interfere the read-out photon with photons from other physical systems, such as cavity quantum electrodynamics[27], ion traps[28] or cavity-enhanced spontaneous parametric down-conversion[29] and so on.

Finally we suppress different decoherence mechanisms to achieve an efficient and long-lived quantum memory. In our experiment, the main sources of decoherence are inhomogeneous broadening due to residual magnetic fields, spin wave dephasing and atoms moving out of the interaction region[5]. To minimize the decoherence caused by the residual magnetic field, we employ the clock states $|g\rangle = |F = 2, m_F = 0\rangle$ and $|s\rangle = |F = 1, m_F = 0\rangle$, which are in the first-order immune to the magnetic field variations. Imperfect pumping to the state $|g\rangle$ gives rise to a slight oscillation of the retrieval efficiency for the short-time (~10 μs) storage. From the relative oscillation amplitude of ~14%, we estimate[6] a pumping efficiency of $p_0 \approx 95\%$, by assuming no occupation in the Zeeman sub-levels $|F = 2, m_F = \pm 2\rangle$. The spin wave dephasing is suppressed by selecting only the forward-scattered write-out photons, which results in a long-wavelength spin wave. After suppressing these two decoherence mechanisms, the remaining dominant decoherence mechanism is the loss of atoms caused by atoms freely flying out of the interaction region. We take two measures to minimize this decoherence. First, we configure the cavity mode in the same direction as the gravity. In this way, the maximal allowed free-falling distance (from the atomic ensemble to the walls of the glass cell) is about 1.5 cm, which corresponds to a falling time of 55 ms. Second, we increase the beam waist of the detection mode from a typical value of 100 μm in previous experiments[5,21] to the present value of 200 μm to reduce the loss of atoms caused by the free expansion of the ensemble. For our temperature of about 10 μK, the estimated lifetime is 4.7 ms.

Experimentally we perform this long-lifetime measurement in a feedback mode (see Methods for details) to save data integration time. In this mode, the write process is repeated until a write-out photon is detected. The read pulse is applied only when a write-out event has been registered. In Fig. 4a, we plot the calibrated retrieval efficiency $R^c$ as a function of the storage time. Note that the dominant decoherence mechanism for short storage time is caused by the imperfect pumping and residual magnetic field[6], and for long storage time is due to atomic motion[5]. Here we fit the data to an exponential function $R_0^c\, e^{-t/\tau}$ for simplicity where $t$ is the storage time, which gives $R_0^c = 79(2)\%$ and $\tau = 3.2(1)$ ms. We attribute the discrepancy between the lifetime $\tau$ and previous theoretical estimations to extra heating during the pumping process. From this fitted value of $R_0^c$ and using $p_r = 0.0094(2)$ and $R = 0.127(3)$ for the first point in Fig. 4a, we calculate the intrinsic spin wave to photon conversion efficiency to be $\chi = 73(2)\%$. We can also see that the quantum memory maintains a retrieval efficiency in excess of 30% for about 3 ms. To further prove that the storage is in the quantum regime, we measure the anti-correlation parameter $\alpha$, which is defined as $\alpha = p_{12}/(p_1 p_2)$ (ref. 30), where $p_1(p_2)$ refers to the detection probability of D1 (D2) in Fig. 1b conditional on a detection event of the write-out photon and $p_{12}$ refers to the conditional coincidence probability between D1 and D2. An ideal

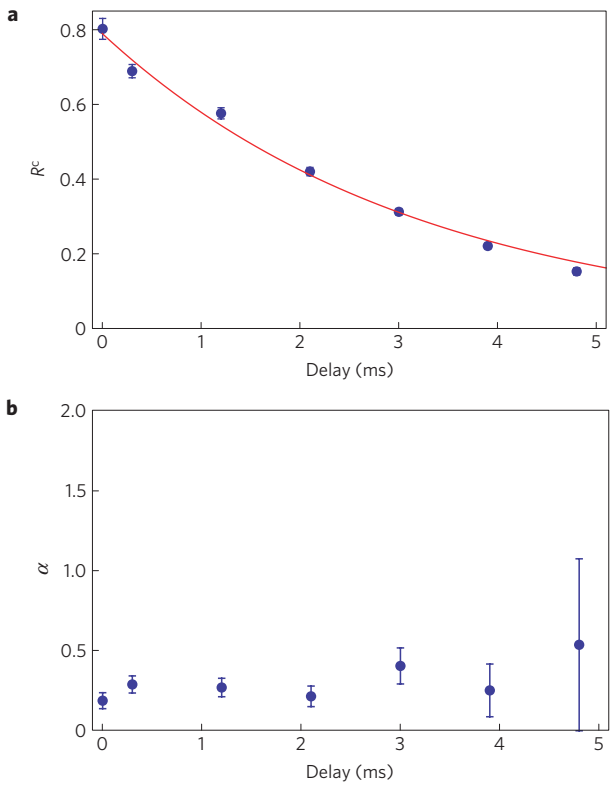


**Figure 4 | Long-lifetime measurement. a**, Calibrated retrieval efficiency $R^c$ as a function of the time delay between read and write. **b**, Anti-correlation parameter $\alpha$ of the conditional read-out photon as a function of the time delay. Error bars are derived on the basis of the Poisson distribution of the detector counts.

single photon corresponds to $\alpha = 0$, whereas for classical light $\alpha = 1$. In our experiment, $\alpha$ is measured as a function of the storage lifetime, with the results shown in Fig. 4b. All of the values are well below the classical bound, which implies that the quantum nature is conserved.

We have realized a high-performance atomic-ensemble quantum memory inside a ring cavity, featuring the simultaneous achievement of a high retrieval efficiency and a long storage lifetime. The lifetime of 3.2 ms is $10^4$ times higher than the duration (about 100 ns) of pulsed optical operations and the retrieval efficiency of 73% is larger than the threshold (50%) of loss-tolerant linear optical quantum computation. The fidelity of the quantum memory is mainly limited by background noise and can be improved by increasing the extinction ratio of pulse switching and single-photon filtering. This realization also enables us to create single photons with much higher source efficiency using the technique of conditional quantum evolution[31]. Further improvement of storage lifetime could be possible by making use of a light-compensated optical lattice[7]. An even further improved retrieval efficiency may be achieved by increasing the pumping efficiency for high optical depths. This demonstration of a high-efficiency and long-lifetime quantum memory enables the implementation of advanced quantum information tasks such as connecting different quantum repeater nodes, the purification[22] of remote entanglement and multi-ensemble entanglement creation.

## Methods

**Technical details.** The repetition rate of our experiment is ~29 Hz. Within each cycle, the first 31.5 ms is used for the MOT loading phase, during which we recapture the atoms and recool them. Afterwards, the experimental phase starts, with a duration between 1 and 4.8 ms determined by the storage time. Within the starting 1 ms of each experimental phase, the write cycle repeats with a repetition rate of 154 kHz (in feedback mode). An optical ring cavity is placed outside the vacuum glass-cell chamber, consisting of one output coupler with a transmission rate of 8.81(3)%, two high-reflection mirrors and two lenses (22.5 cm). The cavity has a round-trip length of 50.3 cm and a free spectral range (FSR) of 595.1 MHz. The glass-cell windows and the lens surfaces are anti-reflection coated. Within one round trip, there is a $\pi$ phase shift between horizontal and vertical polarization, which explains why the ratio of ground-state splitting over one FSR does not equal an integer. The beam waist of the cavity mode can be slightly changed by moving the lens positions.

**Fidelity of the quantum memory.** It can be characterized either by the cross-correlation[5] $g_c^{(2)}$ or the anti-correlation parameter[6] $\alpha$. If the atomic ensemble is used as a single-photon source, the anti-correlation parameter $\alpha$ determines the single-photon quality. If the atomic ensemble is used to implement atom–photon entanglement, the violation of Bell's inequality is characterized by $S > 2$, where $S$ may be expressed as $S \approx 2\sqrt{2}V$ with the visibility $V \approx (g_c^{(2)} - 1)/(g_c^{(2)} + 1)$. Therefore, $g_c^{(2)} \gg 1$ and $\alpha \ll 1$ both demonstrate a high-fidelity quantum memory.

**Cavity enhancement.** The utilization of a ring cavity and configuring it to be quadruple resonant with the write (read) beams and the write-out (read-out) photons offer a series of advantages. First, the intensity of write and read beams inside the cavity is enhanced by a factor of $2F\eta_{esp}/\pi$, which moderates the requirement of single-photon filtering a lot. Second, the ring cavity enhances the emission of the write-out photon into the cavity mode by a factor of $2F/\pi$. Third, and most importantly, the ring cavity enhances the coherent read-out emission by the Purcell effect, which gives rise to a maximal retrieval efficiency[32] of $\chi \approx C/(C+1)$, where the cooperativity $C \propto F \times d$, with $d$ being the optical depth of the atomic ensemble. This relation can be understood as the competition between the collective emission of the read-out field into the cavity mode, which is further enhanced by the Purcell effect, and spontaneous emission into free space through partial population in the excited state.

**Phase shift of the atomic ensemble.** During the spin wave creation and read-out process, most atoms populate in the state $|g\rangle$. Therefore, owing to the close resonance of the write and the read-out photon to the $|g\rangle \rightarrow |e\rangle$ transition, the atomic ensemble will give rise to a phase shift in the write beam and read-out photons. In our experiment this phase shift is measured by monitoring the leakage signal of the write beam from highly reflecting mirror 2 (HR2) as we scan the locking beam centre frequency. To compensate this phase shift (~4°) and achieve the resonance between write (read-out) and the ring cavity mode, we set a frequency offset $\delta$ to the locking beam. Therefore, the locking beam is blue-detuned by one FSR + $\delta$ relative to the write in total. To achieve resonance of the read beam and write-out photons with the ring cavity, we make use of a manual translation stage that is attached to HR2 to change the FSR, and scan its position while monitoring the leakage signal of the read beam from HR2.

**Measurement modes.** We have two different modes for data measurement, that is, correlation mode[5] and feedback mode[6]. In the correlation mode, each write pulse is followed by a read pulse with a fixed delay. In this mode, as $p_w$, $p_r$ and $p_{w,r}$ are measured, we can verify the quantum character of our memory using the cross-correlation $g_c^{(2)}$. In the feedback mode, the write process repeats until a write-out photon is detected. The read pulse is only applied conditioned on these events. In this mode, owing to the unavailability of $p_r$, we measure the anti-correlation parameter $\alpha$ to verify the quantum character.

**Background subtraction.** The background $p_{bg}$ in the write process can be separated into two parts. The first part includes the stray light, the dark count of single-photon detectors and the leakage of the read and locking beam due to the limited extinction ratio of the AOMs, and so on, which are not dependent on the write power and give an overall constant background of 0.0006(1). The second part is mainly due to the leakage of the write laser, which increases linearly as a function of the write power. The write-leakage-induced background contributes ~2.3% of $p_w$. As the write leakage can be further decreased by using more stages of frequency filtering, it is reasonable to subtract this background, which will also enable a more accurate estimate of $\chi$.

Received 18 November 2011; accepted 20 April 2012; published online 20 May 2012

## References

1. Knill, E., Laflamme, R. & Milburn, G. J. A scheme for efficient quantum computation with linear optics. *Nature* **409,** 46–52 (2001).
2. Duan, L-M., Lukin, M. D., Cirac, J. I. & Zoller, P. Long-distance quantum communication with atomic ensembles and linear optics. *Nature* **414,** 413–418 (2001).
3. Simon, J., Tanji, H., Thompson, J. K. & Vuletic, V. Interfacing collective atomic excitations and single photons. *Phys. Rev. Lett.* **98,** 183601 (2007).
4. Hedges, M. P., Longdell, J. J., Li, Y. & Sellars, M. J. Efficient quantum memory for light. *Nature* **465,** 1052–1056 (2010).

5. Zhao, B. *et al.* A millisecond quantum memory for scalable quantum networks. *Nature Phys.* **5,** 95–99 (2009).
6. Zhao, R. *et al.* Long-lived quantum memory. *Nature Phys.* **5,** 100–104 (2009).
7. Radnaev, A. G. *et al.* A quantum memory with telecom-wavelength conversion. *Nature Phys.* **6,** 894–899 (2010).
8. Browne, D. E. & Rudolph, T. Resource-efficient linear optical quantum computation. *Phys. Rev. Lett.* **95,** 010501 (2005).
9. Briegel, H. J., Dur, W., Cirac, J. I. & Zoller, P. Quantum repeaters: The role of imperfect local operations in quantum communication. *Phys. Rev. Lett.* **81,** 5932–5935 (1998).
10. Bodiya, T. P. & Duan, L-M. Scalable generation of graph-state entanglement through realistic linear optics. *Phys. Rev. Lett.* **97,** 143601 (2006).
11. Zhao, B., Chen, Z-B., Chen, Y-A., Schmiedmayer, J. & Pan, J-W. Robust creation of entanglement between remote memory qubits. *Phys. Rev. Lett.* **98,** 240502 (2007).
12. Sangouard, N. *et al.* Robust and efficient quantum repeaters with atomic ensembles and linear optics. *Phys. Rev. A* **77,** 062301 (2008).
13. Varnava, M., Browne, D. E. & Rudolph, T. How good must single photon sources and detectors be for efficient linear optical quantum computation? *Phys. Rev. Lett.* **100,** 060502 (2008).
14. Chaneliere, T. *et al.* Storage and retrieval of single photons transmitted between remote quantum memories. *Nature* **438,** 833–836 (2005).
15. Eisaman, M. D. *et al.* Electromagnetically induced transparency with tunable single-photon pulses. *Nature* **438,** 837–841 (2005).
16. Sherson, J. F. *et al.* Quantum teleportation between light and matter. *Nature* **443,** 557–560 (2006).
17. Saglamyurek, E. *et al.* Broadband waveguide quantum memory for entangled photons. *Nature* **469,** 512–515 (2011).
18. Clausen, C. *et al.* Quantum storage of photonic entanglement in a crystal. *Nature* **469,** 508–511 (2011).
19. Specht, H. P. *et al.* A single-atom quantum memory. *Nature* **473,** 190–193 (2011).
20. Chou, C-W. *et al.* Functional quantum nodes for entanglement distribution over scalable quantum networks. *Science* **316,** 1316–1320 (2007).
21. Yuan, Z-S. *et al.* Experimental demonstration of a BDCZ quantum repeater node. *Nature* **454,** 1098–1101 (2008).
22. Pan, J-W., Simon, C., Brukner, C. & Zeilinger, A. Entanglement purification for quantum communication. *Nature* **410,** 1067–1070 (2001).
23. Barrett, S. D., Rohde, P. P. & Stace, T. M. Scalable quantum computing with atomic ensembles. *New J. Phys.* **12,** 093032 (2010).
24. Kuzmich, A. *et al.* Generation of nonclassical photon pairs for scalable quantum communication with atomic ensembles. *Nature* **423,** 731–734 (2003).
25. Felinto, D., Chou, C. W., de Riedmatten, H., Polyakov, S. V. & Kimble, H. J. Control of decoherence in the generation of photon pairs from atomic ensembles. *Phys. Rev. A* **72,** 053809 (2005).
26. Fleischhauer, M., Imamoglu, A. & Marangos, J. P. Electromagnetically induced transparency: Optics in coherent media. *Rev. Mod. Phys.* **77,** 633–673 (2005).
27. Kimble, H. J. The quantum internet. *Nature* **453,** 1023–1030 (2008).
28. Duan, L. M. & Monroe, C. Colloquium: Quantum networks with trapped ions. *Rev. Mod. Phys.* **82,** 1209–1224 (2010).
29. Bao, X-H. *et al.* Generation of narrow-band polarization-entangled photon pairs for atomic quantum memories. *Phys. Rev. Lett.* **101,** 190501 (2008).
30. Grangier, P., Roger, G. & Aspect, A. Experimental evidence for a photon anticorrelation effect on a beam splitter: A new light on single-photon interferences. *Europhys. Lett.* **1,** 173–179 (1986).
31. Matsukevich, D. N. *et al.* Deterministic single photons via conditional quantum evolution. *Phys. Rev. Lett.* **97,** 013601 (2006).
32. Gorshkov, A. V., André, A., Lukin, M. D. & Sørensen, A. S. Photon storage in Λ-type optically dense atomic media. i. cavity model. *Phys. Rev. A* **76,** 033804 (2007).


## Acknowledgements

This work was supported by the European Commission through the ERC Grant, the STREP project HIP, the CAS, the NNSFC and the National Fundamental Research Program (Grant No. 2011CB921300) of China.

## Author contributions

X-H.B., A.D., B.Z. and J-W.P. conceived and designed the experiment. A.D., P.D., A.R., T.S. and X-H.B. built the set-up. X-H.B., A.R., P.D. and J.R. carried out the experiment. X-H.B., A.R., L.L., N-L.L. and B.Z. analysed the data. X-H.B. and B.Z. wrote the paper with substantial contributions by all authors. J-W.P. supervised the whole project.

## Additional information

The authors declare no competing financial interests. Reprints and permissions information is available online at www.nature.com/reprints. Correspondence and requests for materials should be addressed to B.Z. or J-W.P.